Environ. Sci. Technol. **2006**, *40*, 3787−3793

Iron Isotope Fractionation during Proton-Promoted, Ligand-Controlled, and Reductive Dissolution of Goethite

JAN G. WIEDERHOLD,*,†,‡ STEPHAN M. KRAEMER,† NADYA TEUTSCH,‡,§ PAUL M. BORER,†,§ ALEX N. HALLIDAY,‡,|| AND RUBEN KRETZSCHMAR†

Department of Environmental Sciences, ETH Zurich, CHN, 8092 Zurich, Switzerland, Institute of Isotope Geochemistry and Mineral Resources, ETH Zurich, NW, 8092 Zurich, Switzerland, Swiss Federal Institute of Aquatic Science and Technology (Eawag), 8600 Dübendorf, Switzerland, and Department of Earth Sciences, University of Oxford, Parks Road, Oxford, OX1 3PR, United Kingdom

Iron isotope fractionation during dissolution of goethite (α-FeOOH) was studied in laboratory batch experiments. Proton-promoted (HCl), ligand-controlled (oxalate dark), and reductive (oxalate light) dissolution mechanisms were compared in order to understand the behavior of iron isotopes during natural weathering reactions. Multicollector ICP-MS was used to measure iron isotope ratios of dissolved iron in solution. The influence of kinetic and equilibrium isotope fractionation during different time scales of dissolution was investigated. Proton-promoted dissolution did not cause iron isotope fractionation, concurrently demonstrating the isotopic homogeneity of the goethite substrate. In contrast, both ligand-controlled and reductive dissolution of goethite resulted in significant iron isotope fractionation. The kinetic isotope effect, which caused an enrichment of light isotopes in the early dissolved fractions, was modeled with an enrichment factor for the ^{57}Fe/^{54}Fe ratio of −2.6‰ between reactive surface sites and solution. Later dissolved fractions of the ligand-controlled experiments exhibit a reverse trend with a depletion of light isotopes of ~0.5‰ in solution. We interpret this as an equilibrium isotope effect between Fe(III)−oxalate complexes in solution and the goethite surface. In conclusion, different dissolution mechanisms cause diverse iron isotope fractionation effects and likely influence the iron isotope signature of natural soil and weathering environments.

Introduction

Iron is an essential nutrient for almost all organisms and the Fe(II)/Fe(III) redox couple is a key factor in the regulation of various biogeochemical processes. The biogeochemical iron cycle is closely interlinked with natural cycles of many other nutrient and pollutant elements of environmental interest. Stable isotopes have been very helpful in studying transport and transformation processes of various elements in natural ecosystems (*1*). However, until recently this application was confined mainly to light elements that could be measured in the gas phase (e.g., H, C, O, N, and S). The development of new analytical techniques within the past decade, especially multiple-collector inductively coupled plasma mass spectrometry (MC-ICPMS), has expanded this range to heavier elements (*2*). High-precision data of transition metal isotope ratios in environmental samples are now becoming more and more available, opening up a new, promising, and fast-growing research area of isotope geochemistry (*3*).

Due to its unique importance in natural systems, iron has attracted particular attention (*4*), and iron isotopes now provide a new tool to trace the biogeochemical iron cycle (*5*). Iron has four stable isotopes (percent natural abundance): ^{54}Fe (5.8%), ^{56}Fe (91.8%), ^{57}Fe (2.1%), and ^{58}Fe (0.3%). The δ-notation is commonly used to describe iron isotope fractionation relative to the international iron isotope standard IRMM-014 and is defined as

$$\delta^{56}\mathrm{Fe}\ [‰] = \left(\frac{(^{56}\mathrm{Fe}/^{54}\mathrm{Fe})_{\mathrm{sample}}}{(^{56}\mathrm{Fe}/^{54}\mathrm{Fe})_{\mathrm{IRMM-014}}} - 1\right) \times 10^3$$

or

$$\delta^{57}\mathrm{Fe}\ [‰] = \left(\frac{(^{57}\mathrm{Fe}/^{54}\mathrm{Fe})_{\mathrm{sample}}}{(^{57}\mathrm{Fe}/^{54}\mathrm{Fe})_{\mathrm{IRMM-014}}} - 1\right) \times 10^3$$

The two values can be easily converted into each other by the approximation $\delta^{57}\mathrm{Fe} = 1.5 \times \delta^{56}\mathrm{Fe}$ because the observed fractionation effects are mass-dependent. Variations of δ^{56}Fe in bulk igneous rocks were found to be very small (*6*). In contrast, significant iron isotope variations of more than 1‰ were found in a variety of low-temperature environments including sediments and soils (*7*−*9*). Iron isotope fractionations have been attributed to biotic or abiotic processes including bacterial dissimilatory iron reduction (*10*), precipitation (*11*), and adsorption (*12*) and have been explained by kinetic or equilibrium fractionation effects (*4*−*6*). However, the exact fractionation mechanisms governing the distribution of iron isotopes in nature still remain largely unclear.

Only limited data are available on iron isotope fractionation during abiotic mineral dissolution reactions. No fractionation was observed during hematite dissolution in hydrochloric acid (*13*, *5*). In contrast, significant iron isotope fractionation was observed during dissolution of hornblende in the presence of different organic ligands including oxalate (*14*, *15*). The solution was found to be enriched in light isotopes and the extent of fractionation correlated with the association constants of the organic ligands with ferric iron. The fractionation was attributed predominantly to the retention of heavy iron isotopes in a leached layer that forms on the surface of the hornblende minerals.

Iron isotope ratios from natural soil profiles with pedogenic iron translocation exhibit significant variations (*9*). The light isotopes are preferentially transported during both podzolization in very acidic, oxic soils (ligand-controlled process) and the formation of redoximorphic features in seasonally anoxic soils (redox-controlled process). However, the interpretation of iron isotope field data and the assignment of the observed effects to specific fractionation reactions

---

* Corresponding author phone: +41-(0)44-6336008; fax: +41-(0)44-6331118; e-mail: wiederhold@env.ethz.ch.

† Department of Environmental Sciences, ETH Zurich.

‡ Institute of Isotope Geochemistry and Mineral Resources, ETH Zurich.

§ Swiss Federal Institute of Aquatic Science and Technology (Eawag).

|| University of Oxford.

10.1021/es052228y CCC: $33.50

remain difficult. Therefore, controlled laboratory experiments focusing on single-reaction mechanisms are required to elucidate the key mechanisms of iron isotope fractionation during mineral dissolution.

Goethite (α-FeOOH) is one of the most important Fe oxide minerals in soils and sediments (*16*). It is formed during pedogenesis and weathering. The dissolution behavior of iron oxides such as goethite is a key factor in controlling iron bioavailability for plants and microorganisms (*17*). Iron oxide minerals dissolve by three different mechanisms: proton-promoted, ligand-controlled, and reductive dissolution, which have been studied in detail (*18*, *16*). Proton-promoted dissolution is a slow process except at very acidic pH and plays only a minor role in iron mobilization in nature. The presence of molecules that form stable Fe(III)−ligand complexes (e.g., organic acids and siderophores (*19*, *20*)) can strongly accelerate the dissolution of iron oxides. The ligand molecules adsorb to the iron oxide and form surface complexes (*21*). The subsequent detachment of these surface complexes and release of Fe(III)−ligand complexes represents the rate-limiting step for ligand-controlled dissolution (*18*). In soils and sediments, ligand-controlled dissolution can have a major influence on iron cycling, especially in organic-rich systems (e.g., podzols). The third mechanism, reductive dissolution, is the most important iron oxide dissolution mechanism in nature. Electron transfer to Fe(III) atoms on the oxide surface produces ferrous iron, which is readily released into solution. Reductive dissolution can be mediated by both biotic and abiotic processes. Dissimilatory iron-reducing bacteria couple the oxidation of organic matter to the reduction of iron oxides by using ferric iron as a terminal electron acceptor (*22*). This reaction has been shown to fractionate iron isotopes by producing ferrous iron in solution that is enriched in light isotopes (*10*, *23*). Besides microbially mediated reactions, reductive dissolution of iron oxides can also occur nonenzymatically with a variety of different electron donors (e.g., phenolic compounds (*24*)) and is promoted by photochemical processes (*25*, *26*). In the presence of light, photolysis of Fe(III)−ligand complexes results in electron-transfer reactions and the formation of soluble ferrous iron. Reductive dissolution of iron oxides is strongly accelerated in the presence of ferrous iron or Fe(II)−ligand complexes (*27*).

Oxalate ($C_2O_4^{2-}$) is a ubiquitous organic acid anion and plays an important role in mineral weathering (*28*). It is formed as a product of organic matter decomposition or is exuded by plant roots and microorganisms into soils and weathering environments. Oxalate concentrations in soil solution are highly variable. Typical values are on the order of a few μM but can be as high as several hundreds of μM (*29*). Oxalate can dissolve iron oxides by both ligand-controlled and photochemical reductive dissolution mechanisms. In the dark, oxalate dissolves goethite by a ligand-controlled process releasing Fe(III)−oxalate complexes into solution (*18*). In the presence of light, oxalate dissolves goethite by a photochemical reductive mechanism, producing aqueous Fe(II) and CO_2 (*25*). We have taken advantage of this interesting property of oxalate to study iron isotope fractionation during mineral dissolution by both mechanisms using the same reagent.

The objective of this work is to explore iron isotope fractionation during mineral dissolution by different dissolution mechanisms. We investigated goethite dissolution in batch experiments comparing proton-promoted, ligand-controlled, and reductive dissolution by measuring iron isotope ratios in the dissolved phase. With this approach, we obtain insight into the fractionation mechanisms of iron isotopes during mineral dissolution and contribute to the development of iron isotopes as a tracer for biogeochemical iron cycling in natural systems such as soils.

Experimental Section

Materials and Reagents. Goethite was synthesized following the method of Schwertmann and Cornell (*30*). The crystal structure of the material was checked by powder X-ray diffraction (XRD) and the surface area was determined to be 38 m^2/g (N_2-BET method). The same goethite has been used in previous studies (*17*, *26*). All reagents were p.a. quality and prepared with ultrapure H_2O (>18 MΩ). Polyethylene labware was precleaned with 3 M HNO_3 and rinsed with ultrapure H_2O prior to use. Teflon beakers (Savillex, U.S.) were cleaned with concentrated HNO_3 followed by rinsing with ultrapure H_2O.

Setup of Batch Dissolution Experiments. The ligand-controlled dissolution experiments (oxalate dark) were performed in polyethylene bottles wrapped with aluminum foil. Concentrations of 2.5−5 g/L goethite and 5 mM oxalic acid were used. The pH of the suspension was adjusted to 3.0 at the beginning of the experiment by addition of small amounts of potassium hydroxide. A series of bottles were filled with the well-mixed suspension and then were placed on an overhead shaker. After predefined time steps (5 min to 315 days), bottles were removed from the shaker, centrifuged (3400*g*, 15 min), and carefully decanted. The decanted solution was then immediately filtered through a 0.025 μm cellulose nitrate membrane filter (Schleicher & Schuell, Germany) and acidified with distilled concentrated HNO_3. The pH in the suspension increased to 3.9 after 95 days and to 4.1 after 315 days of dissolution due to the consumption of protons during goethite dissolution. Dissolution was stopped after 315 days. The residue was then washed with water (acidified to pH 4) and afterward leached twice with 0.5 M HCl (leach 1: 15 min; leach 2: 90 min). The remaining residue was totally dissolved in 6 M HCl.

The proton-promoted dissolution experiments were carried out with 0.5 M HCl. A lower pH of ∼0.3 was chosen because proton-promoted dissolution at pH 3 is too slow to produce enough dissolved iron for isotope measurements in a reasonable time frame (*16*). The experimental setup was similar to the oxalate dark experiments. The reaction time ranged from 3 min to 24 h and the goethite solid concentration from 2.5 to 12.5 g/L. The higher solid concentration was necessary to obtain sufficient amounts of iron for isotope analysis from a small dissolved fraction.

The reductive dissolution experiments (oxalate light) were performed in a Pyrex glass vessel that was irradiated by a solar simulator (high-pressure Xenon lamp, OSRAM, Germany), producing a spectrum similar to sunlight and a light energy of 1200 W/m^2 at the sample (*26*). The vessel was water-cooled to constant temperature (25 ± 1 °C), stirred by a magnetic Teflon-coated stirring bar, and constantly purged with nitrogen gas to prevent reoxidation of ferrous iron by oxygen. A lower goethite solid concentration of 0.5 g/L was used to ensure sufficient light penetration. At the beginning of the experiment the oxalic acid concentration was 1 mM. The pH in the suspension increased from 3.0 to 5.1 at the end of the experiment. Adsorption of Fe(II) to the goethite surface is negligible below pH 5 (*31*), which is important as adsorption reactions could induce additional isotope fractionation effects (*12*). The suspension was sampled with a syringe after predefined dissolution times (5 min to 7.5 h), immediately filtered (0.025 μm), and acidified with HNO_3.

Finally, the remaining goethite solid material of all dissolution experiments and the unreacted goethite were completely dissolved in 6 M HCl to measure the iron isotope composition of the bulk solid and to assess the isotopic homogeneity of the goethite material.

Sample Preparation for Isotope Analysis. Sample preparation took place in a clean chemistry laboratory and the detailed methods have been previously described (*12*).

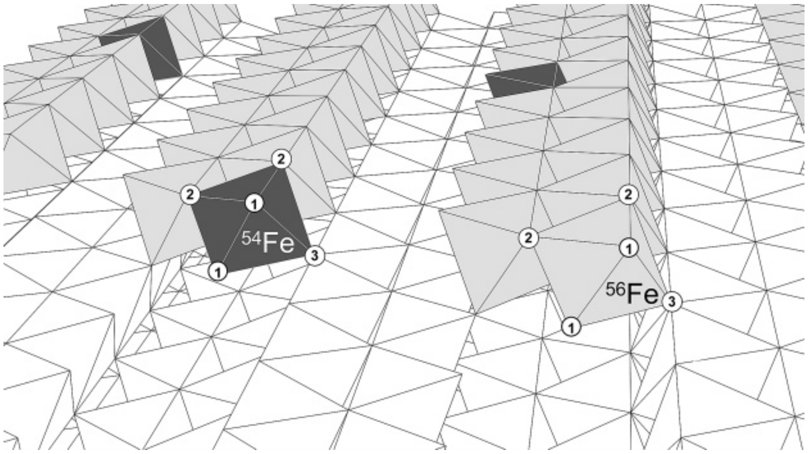

FIGURE 1. Dissolution of goethite at monatomic steps (modified after ref *37*). Iron is octahedrally coordinated to six oxygen atoms that are partially protonated. Dissolution proceeds at monatomic steps along double chains of ^{54}Fe (black) and ^{56}Fe (grey) octahedra at the mineral surface (^{57}Fe and ^{58}Fe are not considered for simplicity). Bulk Fe octahedra below are shown in white without indication of isotopic masses. Bidentate ligands such as oxalate can only attack iron octahedra with at least two singly coordinated oxygens (marked as 1) (*38*). These dissolution active sites constitute only a small fraction of the total surface sites. Iron isotope ratios in solution only change if doubly and triply coordinated oxygen atoms (marked at 2 and 3) remain at the surface, i.e., if bonds between the detaching iron atom and 2 and 3 are broken in the dissolution reaction. In this case, dissolution of ^{54}Fe sites proceeds faster than dissolution of ^{56}Fe sites.

Sample solutions (up to 240 mL) were evaporated on a hotplate in Teflon beakers and treated several times with 30% H_2O_2 and concentrated HNO_3 to oxidize oxalate to CO_2 and ferrous iron to ferric iron. Subsequently, the samples were redissolved in 6 M HCl, purified in Teflon columns on anion-exchange resin (Bio-Rad AG1 X4, 200−400 mesh) with quantitative recovery, again evaporated, and finally diluted to 8 ppm Fe in 0.05 M HCl.

Analytical Methods. Iron concentrations were measured by atomic absorption spectrometry (AAS, SpectrAA 220, Varian, Australia). Iron isotope ratios were measured by multiple-collector inductively coupled plasma mass spectrometry (MC-ICPMS, Nu Plasma, Nu instruments, U.K.). The analytical procedures for iron isotope measurement have been previously described in detail (*12*, *32*). Briefly, a standard-bracketing approach with IRMM-014 was used to correct for machine drift and instrumental mass bias (*33*). A membrane desolvation system (MCN-6000, Cetac, U.S.) was used to minimize argide interferences (ArN^+, ArO^+, and $ArOH^+$) to insignificant levels (background-to-signal ratio typically <0.001). The ^{57}Fe/^{54}Fe and ^{56}Fe/^{54}Fe ratios were measured simultaneously and all data plotted on the theoretical mass fractionation line demonstrating the absence of isobaric interferences. A Cr correction was performed by monitoring mass 52 or 53 to calculate the potential influence of ^{54}Cr on ^{54}Fe. However, our purified solutions did not contain significant amounts of Cr and the Cr-corrected and uncorrected δ^{57}Fe values differed by less than ±0.01‰. All masses were collected in Faraday cups equipped with 10^{11} Ω resistors except mass 56, which was collected in a Faraday cup equipped with a 10^9 Ω resistor. This allowed solutions to be run with relatively high Fe concentrations (8 ppm) but it affected the precision of the ^{56}Fe/^{54}Fe measurement. Therefore, due to the smaller analytical error for the ^{57}Fe/^{54}Fe ratio, the results are expressed as δ^{57}Fe with a long-term reproducibility of $\pm\leq 0.15‰$ (2SD). Samples were only measured after several stable isotope measurements of an internal house standard against IRMM-014. This standard was again measured after every six samples and at the end of the analytical run. All data in this paper are reported as Δ^{57}Fe relative to the isotopic composition of the bulk goethite ($\Delta^{57}\mathrm{Fe} = \delta^{57}\mathrm{Fe}_{\mathrm{IRMM}} - \delta^{57}\mathrm{Fe}_{\mathrm{bulkgoethite}}$), which has a δ^{57}Fe value of $+0.54 \pm 0.15‰$ ($n = 11$) and was processed identically to all other samples.

Modeling Approach. Isotope fractionation during dissolution cannot be described by a simple Rayleigh fractionation model because dissolution reactions only proceed at the surface of the mineral. Therefore, only a small pool of the substrate participates in the reaction at any given time. The size of the total surface site pool (i.e., one monolayer) of the goethite was calculated from the N_2-BET surface area (38 m^2/g) combined with an estimated surface site density of 4.35 Fe atoms/nm^2 based on a detailed study of goethite surface structure (*34*) considering that the (010) face is the most relevant goethite surface for dissolution (*35*). Accordingly, the total surface site pool makes up ~2.4% of the total iron atoms in the goethite. Furthermore, dissolution of surface atoms from a mineral such as goethite is dominated by a subset of highly reactive surface sites (*36*). Specifically, monatomic steps on the surface expose iron octahedra that are not fully coordinated and more susceptible to proton or ligand attack (Figure 1, *37*). These reactive sites are self-reproducing because new octahedra are constantly exposed as dissolution proceeds along double chains of iron (oxy)-hydroxide octahedra. The rate of dissolution of an exposed octahedron may be influenced by the isotopic mass of the central iron atom. If one isotope is preferentially dissolved, the other isotopes are subsequently enriched on the remaining surface while the bulk of the mineral phase remains unchanged. We developed a kinetic fractionation model based on dissolution of reactive surface sites that accounts for this surface-enrichment effect. Our model is conceptually similar to the model used by Brantley et al. to describe the distribution of ^{56}Fe and ^{54}Fe within a leached layer at the surface of hornblende minerals (*15*). While goethite does not develop a leached layer, iron isotope fractionation occurs between a reactive surface site pool of constant size and the solution. Our model considers all four iron isotopes (^{54}Fe, ^{56}Fe, ^{57}Fe, and ^{58}Fe) with their relative mass differences, abundances, and interactions. We modeled the dissolution of the reactive surface site pool (rss) with a preferential release of the lighter isotopes (fixed enrichment factor $\varepsilon = \Delta^{57}\mathrm{Fe}_{\mathrm{sol}} - \Delta^{57}\mathrm{Fe}_{\mathrm{rss}}$) and subsequent replenishment of the depleted residual reactive surface site pool with unfractionated bulk material. A detailed description of our model is provided in the Supporting Information.

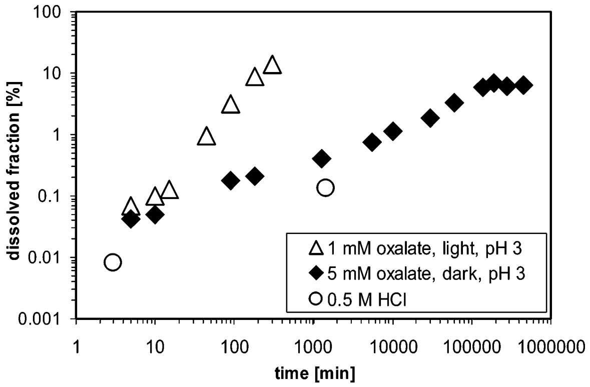

FIGURE 2. Dissolution of goethite during the three batch experiments. The dissolved fraction in the oxalate dark experiments (ligand-controlled dissolution) did not increase after about 4 months of reaction, indicating that the solution was saturated and a chemical equilibrium approached.

Results and Discussion

Dissolution Kinetics. The dissolution kinetics of goethite during proton-promoted (0.5 M HCl), ligand-controlled (oxalate dark), and reductive dissolution (oxalate light) are illustrated in Figure 2. Proton-promoted dissolution was the slowest process, even at the lower pH of ~0.3 compared to pH 3 in the other two experiments. Reductive dissolution (oxalate light) exhibited by far the fastest dissolution rate, achieving a dissolved fraction of 13.8% in 5 h, whereas ligand-controlled dissolution dissolved only 6.3% of the goethite in 315 days. An amount of iron corresponding to a single surface monolayer (~2.4% of total Fe) dissolved in less than 90 min by reductive dissolution and in about 4 weeks by ligand-controlled dissolution. Dissolution rates changed slightly over the course of the experiments. The increase in dissolution rate in the oxalate light experiments can be explained by the autocatalytic effect of increasing ferrous iron concentrations on the reductive dissolution (*25*, *27*). A decrease in reaction rates at the end of the oxalate dark experiments occurred as the reaction approached chemical equilibrium.

Iron Isotopes. Figure 3 shows the iron isotope composition in solution as a function of the dissolution time. It is important to note that all data points show accumulated values because samples were taken from independent parallel bottles (0.5 M HCl and oxalate dark) or from one batch where only small aliquots were sampled over time (oxalate light). Therefore, the iron isotope ratio in solution at a given time represents the average of dissolved iron up to the sampling time. In the 0.5 M HCl experiments, Δ^{57}Fe in solution did not vary between dissolved fractions and was not statistically different from the bulk value obtained by total dissolution in 6 M HCl. Hence, proton-promoted dissolution with 0.5 M HCl does not induce fractionation of iron isotopes. This result is in agreement with previous studies on hematite dissolution by HCl where no iron isotope fractionation was reported (*5*, *13*) and confirms that the goethite is not isotopically zoned.

In contrast, both ligand-controlled and reductive dissolution experiments result in significant fractionation of iron isotopes. To interpret these data, the course of the dissolution process is divided into an early and a late stage. The early dissolved fractions show a strong enrichment in the light isotope ^{54}Fe with Δ^{57}Fe values of −1.8‰ and −2.5‰ in the ligand-controlled and reductive dissolution experiments, respectively. A faster dissolution rate of light ^{54}Fe atoms compared to heavier ^{57}Fe atoms can explain the observed Δ^{57}Fe values in solution. This effect diminishes over the course of the experiment and Δ^{57}Fe values gradually increase toward the isotopic composition of the bulk goethite (0‰) in later dissolved fractions. Preferential dissolution of light isotopes concurrently causes the remaining surface (and only the surface) to become depleted in light isotopes. Dissolution of a progressively heavier substrate results in the release of increasingly heavier iron from the surface until the released iron has the same isotopic composition as the bulk mineral phase at steady-state conditions (*15*), while the reactive surface sites are enriched in heavy isotopes.

Model Results. Figure 4 shows the model results of the kinetic isotope effect in the early-stage dissolution where Δ^{57}Fe is plotted as a function of dissolved fraction. We achieved the best fit for both ligand-controlled and reductive dissolution experiments using an enrichment factor ε of −2.6‰ for the ^{57}Fe/^{54}Fe ratio. This corresponds to −1.7‰ for the ^{56}Fe/^{54}Fe ratio. The size of the reactive surface site pool was fitted to be 2.4% and 5.9% of the monolayer for ligand-controlled and reductive dissolution, respectively. The higher value for the oxalate light experiments seems to indicate that photochemical reductive dissolution could

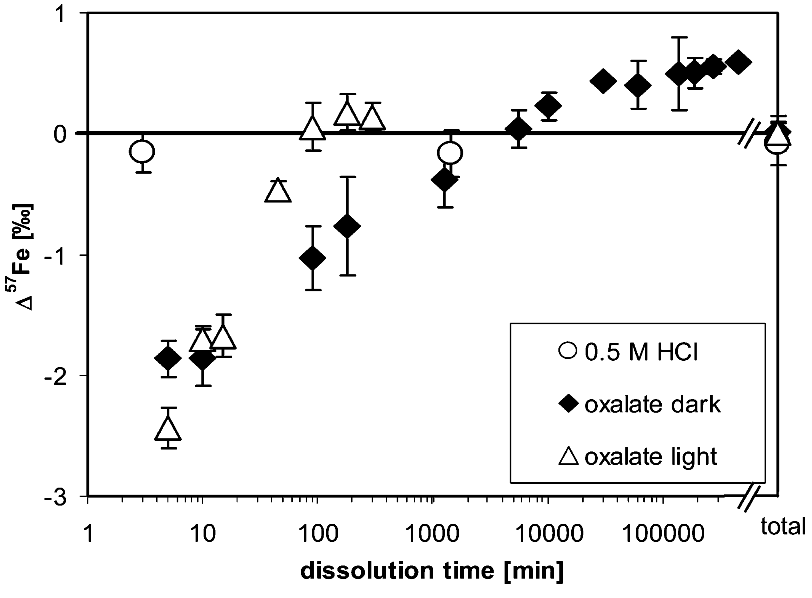

FIGURE 3. Iron isotopes in solution as a function of the dissolution time. Total dissolution of remaining solids was achieved in 6 M HCl. Error bars indicate 2SD of replicate measurements ($n = 3-6$). Δ^{57}Fe describes iron isotope fractionation relative to the bulk goethite ($\Delta^{57}Fe = \delta^{57}Fe_{IRMM} - \delta^{57}Fe_{bulkgoethite}$).

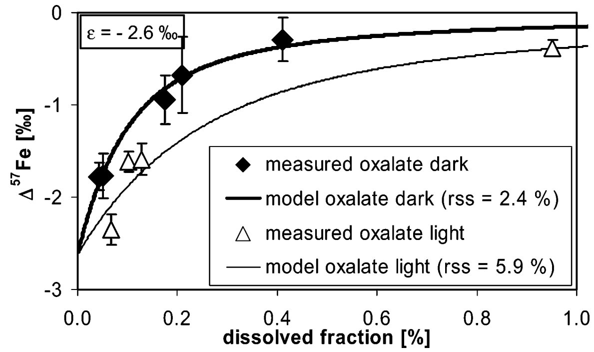

FIGURE 4. Modeling results of kinetic isotope effect during early dissolved fraction. The best fit was achieved with an enrichment factor ε of −2.6‰ and a size of the reactive surface site pool (rss) of 2.4% of the surface monolayer for the oxalate dark experiments (ligand-controlled dissolution) and 5.9% for the oxalate light experiments (reductive dissolution). A detailed description of the model is presented in the Supporting Information.

occur on crystallographic sites that are not reactive in ligand-controlled dissolution. For example, ferrous iron released during reductive dissolution may form ternary surface complexes to oxalate adsorbed to the goethite surface (*27*) and electron transfer through the bridging ligand could result in reduction and subsequent release of Fe atoms at the goethite surface even from less labile crystallographic positions. The lack of independent information about the exact size of the reactive surface site pool certainly restricts the precision of our model. Information on the sensitivity of our model toward the size of the reactive surface site pool and the enrichment factor can be found in the Supporting Information. The resulting enrichment factor of −2.6‰ for both ligand-controlled and reductive dissolution corresponds to a fractionation factor $\alpha_{\text{goethite-solution}}$ of 1.0026 for the ^{57}Fe/^{54}Fe ratio. The enrichment factor equals Δ^{57}Fe in solution at the onset of the dissolution reaction. Our first samples were taken when surface depletion of the light isotope was already ongoing. However, Δ^{57}Fe values of the first dissolved fractions (−1.8‰ for oxalate dark and −2.5‰ for oxalate light) provide minimum estimates for the enrichment factor.

Fractionation Mechanism. The close proximity of iron isotope fractionation factors in ligand-controlled and reductive dissolution is interesting considering the different mechanisms and end products of the reactions. Ligand-controlled dissolution releases Fe(III)−ligand complexes into solution whereas reductive dissolution produces aqueous Fe(II). However, in both cases the rate-determining step is the detachment of the dissolving iron ions from the goethite surface. We propose that this step is responsible for the observed kinetic iron isotope fractionation. Several Fe−O bonds of the goethite lattice have to be broken during the detachment of iron from the surface (Figure 1). The bond energy differs between different iron isotopes and it is energetically easier to break a bond with a lighter ^{54}Fe isotope. This effect can explain the enrichment of light iron isotopes in solution during the kinetically controlled early-stage dissolution. However, Δ^{57}Fe in solution can only change if the mass of the detaching iron atom is causing the isotope effect. If the detaching iron atom carries along its coordinating oxygens of the lattice, i.e., if the detachment involves breaking of the bonds between the coordinating oxygen and adjacent iron atoms, no isotope fractionation is expected because the isotopic mass of the detaching iron has little effect on the bond breakage. The difference of iron isotope fractionation in proton-promoted and ligand-controlled dissolution may therefore be a consequence of differences in the nature of the bond exchange mechanism. Ligands such as oxalate directly attack the detaching iron atom, thereby weakening the bonds between the detaching iron atom and coordinating oxygen atoms (*38*). We suggest that this induces breakage of these bonds and results in iron isotope fractionation. However, protonation of lattice oxygen atoms weakens the bonds to both detaching and adjacent iron atoms. It is unknown whether the detaching or remaining iron atoms get oxygen atoms from dissociating water molecules to reconstitute the octahedral coordination sphere of iron during proton-promoted dissolution (*37*). Lack of observed iron isotope fractionation may indicate bond breakage between oxygen and adjacent iron atoms during detachment.

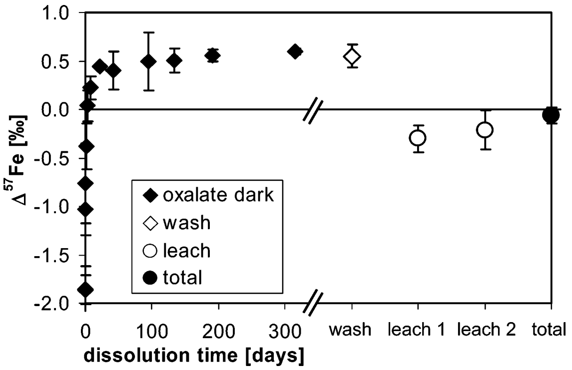

FIGURE 5. Late-stage dissolution (oxalate dark) and leaching experiment. Dissolution was stopped after 315 days. The residue was washed with water (acidified to pH 4) and afterward leached twice with 0.5 M HCl (leach 1: 15 min; leach 2: 90 min). The remaining residue was totally dissolved in 6 M HCl. Negative Δ^{57}Fe values of leach samples indicate the presence of an isotopically light surface iron pool. This is consistent with the concept of equilibrium isotope fractionation between "heavy" Fe(III)−oxalate complexes in solution and a "light" goethite surface.

Brantley et al. (*15*) reported no significant iron isotope fractionation during ligand-controlled goethite dissolution in the presence of a siderophore, which was based on iron isotope measurements from a single dissolved fraction. Considering the evolution of Δ^{57}Fe in solution during dissolution, the results depend heavily on the sampling strategy and it is difficult to compare their results with ours.

Late-Stage Dissolution. The kinetic fractionation model only explains the data of the early dissolved fractions within one surface monolayer. The model predicts the convergence of the iron isotope ratio in solution with the composition of the bulk solid (Δ^{57}Fe = 0‰) as the reaction proceeds. However, we observed an increase of Δ^{57}Fe in solution with increasing dissolution time exceeding the value of the bulk goethite (Figure 3). The solution of the ligand-controlled experiments (oxalate dark) reaches a plateau of Δ^{57}Fe at approximately +0.5‰ relative to the bulk goethite. A similar but smaller effect was observed during the reductive dissolution (oxalate light) with Δ^{57}Fe values of about +0.2‰.

Solubility calculations of Fe(III)−oxalate indicated that chemical equilibrium in our system was not reached before approximately three surface monolayers were dissolved (solubility and hydrolysis constants taken from ref *20*). However, no significant change in the isotopic composition of the solution was observed between the dissolution of the first surface monolayer (after 4 weeks) and the last measurement (after 315 days) when the system was very close to chemical equilibrium. Therefore, the attainment of the Δ^{57}Fe plateau value in solution of +0.5‰ in the ligand-controlled experiments did occur somewhat before the chemical equilibrium of the dissolution reaction was reached. However, the time scales to reach chemical and isotopic equilibrium can differ substantially (*6*, *39*). Mass balance considerations dictate that if the solution is enriched in heavy isotopes, the mineral surface must be enriched in light isotopes. Figure 5 shows the results of the leaching experiment with 0.5 M HCl that was performed at the end of the oxalate dark experiments after 315 days. Negative Δ^{57}Fe values in the leach solutions indicate the presence of an isotopically light surface iron pool on the goethite surface. In any case, the enrichment of heavy isotopes in the product of the reaction and the constant solution value over very long time periods (several months) suggests that equilibrium isotope fractionation rather than a kinetic effect is dominating the late-stage dissolution of the ligand-controlled experiment.

Kinetic isotope effects can only be observed in incomplete and unidirectional reactions (*1*). However, if the dissolution reaction is approaching equilibrium and the back reaction is gaining in importance, kinetic isotope effects will eventually disappear. Then equilibrium isotope fractionation sets in, which is governed by energetic differences in the bonding environment of the reactant and the product (*1*). Isotope fractionation theory predicts that equilibrium fractionation enriches the heavier isotope in the stronger bonding environment (*40*). It is possible that kinetic and equilibrium fractionation in the same system result in opposite effects especially if the product of the reaction provides a stronger bonding environment compared to the reactant. This seems to be the case for ligand-controlled dissolution where the main driving force of the reaction is the formation of iron−ligand complexes. Iron(III)−oxalate complexes in solution probably provide a stronger bonding environment than the goethite surface, causing an enrichment of heavy isotopes in the product of the reaction and positive Δ^{57}Fe values in solution. Consequently, an equilibrium isotope effect dominates during late-stage dissolution, leading to the enrichment of the heavy isotopes in solution. This hypothesis is supported by the observation of an isotopically light surface iron pool during the leach experiments. However, further work is certainly needed to confirm the equilibrium isotope effect. It is probable that different ligand complexes could have different equilibrium fractionation factors.

Environmental Significance. The dissolution of kinetically stable mineral phases in soils is often sustained by persistent strong disequilibria with the soil solution. Thus, it can be assumed that kinetic isotope effects dominate during dissolution reactions of iron oxide minerals in soils and sediments especially if a physical separation of reactant and product is taking place. However, it is possible that under certain conditions equilibrium fractionation effects become important in nature. Our finding of an inverse fractionation effect between kinetic early-stage and equilibrium late-stage processes during mineral dissolution may have important implications for the interpretation of iron isotope data in natural systems such as soils with highly heterogeneous solution chemistry at a small scale. In addition, our results indicate that oxalate extractions, which are widely used to separate poorly crystalline iron oxides from soil or sediment samples (*16*), are inappropriate for iron isotope studies. Extractions with 0.5 M HCl should be preferred due to the absence of isotope fractionation artifacts during the procedure. In summary, we have demonstrated that iron isotopes are significantly fractionated during dissolution of goethite by ligand-controlled and reductive dissolution, but not by proton-promoted dissolution. This work provides a detailed examination of iron isotope fractionation during mineral dissolution by different mechanisms. Our results will help to further develop iron isotopes as a powerful tool for the study of the biogeochemical iron cycle in nature.

Acknowledgments

We thank Kurt Barmettler for support in the laboratory, Nicholas Chambers for help during sampling and sample preparation, and the staff of the ETH MC-ICPMS lab for excellent maintenance and support. Ariel Anbar, Thomas Bullen, and two anonymous reviewers are thanked for their helpful comments. This research was funded by ETH Research Grant No. 01927.

Note Added after ASAP Publication

Some characters in the caption of Figure 3 appeared incorrectly in the version published on the web May 19, 2006. These have been corrected in the version published May 23, 2006.

Supporting Information Available

The Supporting Information contains additional data tables and a detailed model description. This material is available free of charge via the Internet at http://pubs.acs.org.

Literature Cited

(1) Hoefs, J. *Stable isotope geochemistry*, 5th ed.; Springer: Berlin, 2004.

(2) Halliday, A. N.; Lee, D.-C.; Christensen, J. N.; Rehkämper, M.: Yi, W.; Luo, X.; Hall, C. M.; Ballentine, C. J.; Pettke, T.; Stirling, C. Applications of multiple collector-ICPMS to cosmochemistry, geochemistry, and paleoceanography. *Geochim. Cosmochim. Acta* **1998**, 919−940.

(3) Johnson, C. M., Beard, B. L., Albarède, F., Eds. *Geochemistry of non-traditional stable isotopes*; Reviews in Mineralogy and Geochemistry 55; Mineralogical Society of America and Geochemical Society: Washington, DC, 2004.

(4) Anbar, A. D. Iron stable isotopes: beyond biosignatures. *Earth Planet. Sci. Lett.* **2004**, *217*, 223−236.

(5) Johnson, C. M.; Beard, B. L.; Roden, E. E.; Newman, D. K.; Nealson, K. H. Isotopic constraints on biogeochemical cycling of Fe. *Rev. Mineral. Geochem.* **2004**, *55*, 359−408.

(6) Beard, B. L.; Johnson, C. M. Fe isotope variations in the modern and ancient Earth and other planetary bodies. *Rev. Mineral. Geochem.* **2004**, *55*, 319−357.

(7) Fantle, M. S.; DePaolo, D. J. Iron isotope fractionation during continental weathering. *Earth Planet. Sci. Lett.* **2004**, *228*, 547−562.

(8) Matthews, A.; Morgans-Bell, H. S.; Emmanuel, S.; Jenkyns, H. C.; Erel, Y.; Halicz L. Controls on iron-isotope fractionation in organic-rich sediments (Kimmeridge Clay, Upper Jurassic, Southern England). *Geochim. Cosmochim. Acta* **2004**, *68*, 3107−3123.

(9) Wiederhold, J. G.; Teutsch, N.; Kretzschmar, R.; Kraemer, S. M.; Halliday, A. N. Iron isotope fractionation during soil formation − comparison of ligand and redox controlled processes. *Geochim. Cosmochim. Acta* **2004**, *68*, 11S:A415.

(10) Beard, B. L.; Johnson, C. M.; Cox, L.; Sun, H.; Nealson, K. H.; Aguilar C. Iron isotope biosignatures. *Science* **1999**, *285*, 1889−1892.

(11) Bullen, T. D.; White, A. F.; Childs, C. W.; Vivit, D. V.; Schulz, M. S. Demonstration of significant abiotic iron isotope fractionation in nature. *Geology* **2001**, *29*, 699−702.

(12) Teutsch, N.; von Gunten, U.; Porcelli, D.; Cirpka, O. A.; Halliday, A. N. Adsorption as a cause for iron isotope fractionation in reduced groundwater. *Geochim. Cosmochim. Acta* **2005**, *69*, 4175−4185.

(13) Skulan, J. L.; Beard, B. L.; Johnson, C. M. Kinetic and equilibrium Fe isotope fractionation between aqueous Fe(III) and hematite. *Geochim. Cosmochim. Acta* **2002**, *66*, 2995−3015.

(14) Brantley, S. L.; Liermann, L.; Bullen, T. D. Fractionation of Fe isotopes by soil microbes and organic acids. *Geology* **2001**, *29*, 535−538.

(15) Brantley S. L.; Liermann L. J.; Guynn R. L.; Anbar A.; Icopini G. A.; Barling J. Fe isotopic fractionation during mineral dissolution with and without bacteria. *Geochim. Cosmochim. Acta* **2004**, *68*, 3189−3204.

(16) Cornell, R. M.; Schwertmann, U. *The iron oxides − structure, properties, reactions, occurrence and uses*, 2nd ed.; VCH: Weinheim, 2003.

(17) Reichard, P. U.; Kraemer, S. M.; Frazier, S.; Kretzschmar, R. Goethite dissolution in the presence of phytosiderophores: rates, mechanisms, and the synergistic effect of oxalate. *Plant Soil* **2005**, *276*, 115−132.

(18) Zinder, B.; Furrer, G.; Stumm, W. The coordination chemistry of weathering: II. Dissolution of Fe(III) oxides. *Geochim. Cosmochim. Acta* **1986**, *50*, 1861−1869.

(19) Cheah, S. F.; Kraemer, S. M.; Cervini-Silva, J.; Sposito, G. Steady-state dissolution kinetics of goethite in the presence of des-

ferrioxamine B and oxalate ligands: implications for the microbial acquisition of iron. *Chem. Geol.* **2003**, *198*, 63−75.

(20) Kraemer, S. M. Iron oxide dissolution and solubility in the presence of siderophores. *Aquat. Sci.* **2004**, *66*, 3−18.

(21) Persson, P.; Axe, K. Adsorption of oxalate and malonate at the water-goethite interface: molecular surface speciation from IR spectroscopy. *Geochim. Cosmochim. Acta* **2005**, *69*, 541−552.

(22) Lovley, D. R.; Holmes, D. E.; Nevin, K. P. Dissimilatory Fe(III) and Mn(IV) reduction. *Adv. Microb. Physiol.* **2004**, *49*, 219−286.

(23) Crosby, H. A.; Johnson, C. M.; Roden, E. E.; Beard, B. L. Coupled Fe(II)-Fe(III) electron and atom exchange as a mechanism for Fe isotope fractionation during dissimilatory iron oxide reduction. *Environ. Sci. Technol.* **2005**, *39*, 6698−6704.

(24) LaKind, J. S.; Stone, A. T. Reductive dissolution of goethite by phenolic reductants. *Geochim. Cosmochim. Acta* **1989**, *53*, 961−971.

(25) Sulzberger, B.; Laubscher, H. Reactivity of various types of iron(III) (hydr)oxides towards light-induced dissolution. *Mar. Chem.* **1995**, *50*, 103−115.

(26) Borer, P. M.; Sulzberger, B.; Reichard, P.; Kraemer, S. M. Effect of siderophores on the light-induced dissolution of colloidal iron(III) (hydr)oxides. *Mar. Chem.* **2005**, *93*, 179−193.

(27) Suter, D.; Siffert, C.; Sulzberger, B.; Stumm, W. Catalytic dissolution of iron(III) (hydr)oxides by oxalic acid in the presence of Fe(II). *Naturwissenschaften* **1988**, *75*, 571−573.

(28) Drever, J. I.; Stillings, L. L. The role of organic acids in mineral weathering. *Colloids Surf., A* **1997**, *120*, 167−181.

(29) Jones, D. L. Organic acids in the rhizosphere − a critical review. *Plant Soil* **1998**, *205*, 25−44.

(30) Schwertmann, U.; Cornell, R. M. *Iron oxides in the laboratory − preparation and characterization*, 2nd ed.; Wiley-VCH: Weinheim, 2000.

(31) Silvester, E.; Charlet, L.; Tournassat, C.; Géhin, A.; Grenèche, J.-M.; Liger, E. Redox potential measurements and Mössbauer spectrometry of Fe^{II} adsorbed onto Fe^{III} (oxyhydr)oxides. *Geochim. Cosmochim. Acta* **2005**, *69*, 4801−4815.

(32) Williams, H. M.; McCammon, C. A.; Peslier, A. H.; Halliday, A. N.; Teutsch, N.; Levasseur, S.; Burg, J.-P. Iron isotope fractionation and the oxygen fugacity of the mantle. *Science* **2004**, *304*, 1656−1659.

(33) Schoenberg, R.; von Blanckenburg, F. An assessment of the accuracy of stable Fe isotope ratio measurements on samples with organic and inorganic matrices by high-resolution multicollector ICP-MS. *Int. J. Mass. Spectrom.* **2005**, *242*, 257−272.

(34) Koretsky, C. M.; Sverjensky, D. A.; Sahai, N. Surface site types on oxide and silicate minerals based on crystal chemistry: Implications for site types and densities, multi-site adsorption, surface infrared spectroscopy, and dissolution kinetics. *Am. J. Sci.* **1998**, *298*, 349−438.

(35) Cornell, R. M.; Posner, A. M.; Quirk, J. P. Crystal morphology and the dissolution of goethite. *J. Inorg. Nucl. Chem.* **1974**, *36*, 1937−1946.

(36) Wehrli, B.; Wieland, E.; Furrer, G. Chemical mechanisms in the dissolution kinetics of minerals; the aspect of active sites. *Aquat. Sci.* **1990**, *52*, 3−31.

(37) Casey, W. H.; Ludwig, C. The mechanism of dissolution of oxide minerals. *Nature* **1996**, *381*, 506−509.

(38) Holmen, B. A.; Casey, W. H. Hydroxamate ligands, surface chemistry, and the mechanism of ligand-promoted dissolution of goethite [α-FeOOH(s)]. *Geochim. Cosmochim. Acta* **1996**, *60*, 4403−4416.

(39) Barling, J.; Anbar, A. D. Molybdenum isotope fractionation during adsorption by manganese oxides. *Earth Planet. Sci. Lett.* **2004**, *217*, 315−329.

(40) Schauble, E. Applying stable isotope fractionation theory to new systems. *Rev. Mineral. Geochem.* **2004**, *55*, 65−111.

Received for review November 7, 2005. Revised manuscript received April 13, 2006. Accepted April 17, 2006.

ES052228Y